Photodegradation of indigo carmine and methylene blue dyes in aqueous solution by SiC–TiO$_2$ catalysts prepared by sol–gel

Christian Gómez-Solís [a], Isaías Juárez-Ramírez [b,*], Edgar Moctezuma [a], Leticia M. Torres-Martínez [b]

[a] Facultad de Ciencias Químicas, Universidad Autónoma de San Luis Potosí, San Luis Potosí Av. Manuel Nava #6, San Luis Potosí, S.L.P. 78290, Mexico
[b] Departamento de Ecomateriales y Energía, Facultad de Ingeniería Civil, Universidad Autónoma de Nuevo León, Cd. Universitaria, San Nicolás de los Garza, Nuevo León 66450, Mexico

ARTICLE INFO

ABSTRACT

Indigo carmine and methylene blue dyes in aqueous solution were photodegraded using SiC–TiO$_2$ catalysts prepared by sol–gel method. After thermal treatment at 450 °C, SiC–TiO$_2$ catalysts prepared in this work showed the presence of SiC and TiO$_2$ anatase phase. Those compounds showed specific surface area values around 22–25 m^2 g^{-1}, and energy band gap values close to 3.05 eV. In comparison with TiO$_2$ (P25), SiC–TiO$_2$ catalysts showed the highest activity for indigo carmine and methylene blue degradation, but this activity cannot be attributed to the properties above mentioned. Therefore, photocatalytic performance is due to the synergy effect between SiC and TiO$_2$ particles caused by the sol–gel method used to prepare the SiC–TiO$_2$ catalysts. TiO$_2$ nanoparticles are well dispersed onto SiC surface allowing the transfer of electronic charges between SiC and TiO$_2$ semiconductors, which avoid the fast recombination of the electron–hole pair during the photocatalytic process.

© 2012 Elsevier B.V. All rights reserved.

1. Introduction

Photodegradation of organic pollutants by heterogeneous photocatalysis has attracted considerable attention in the last few decades because through this method it is possible to carry out the photocatalytic oxidation of an organic substance causing its partial or total mineralization [1]. During the photocatalytic process, electron–hole pairs are generated in valence and conduction bands of a semiconductor, provoking on its surface the presence of radicals, which attack the molecules of pollutants [1]. Commonly, TiO$_2$ is the commercial semiconductor commonly used in photocatalysis due to its cost effectiveness, inert nature and photostability [1,2]. However, one of the most important problems detected is the fast recombination of photogenerated electron–hole pairs [3,4] which decreases the photocatalytic activity of this material. Another problem is that its use in industrial applications has some limitations like its difficulty to recover it after the photocatalytic reaction. In view of that, it is a convenient inert support to attach this material with strong adherence and high chemical stability. In this sense, several materials have been used as support for TiO$_2$, such as glasses, silica gel, quartz sands, carbon active, ITO glasses, Al$_2$O$_3$, SiC [5–11]. However in almost all cases TiO$_2$ activity is lost after its deposition.

SiC has been considered as support due to its properties such as high thermal conductivity, high mechanical strength, as well as its low chemical reactivity [6]. Fe$_2$O$_3$ and TiO$_2$ nanoparticles have been deposited on SiC surface showing high photocatalytic activity for the dehydrogenation of ethanol to acetaldehyde [7], methylethylacetone oxidation [8], and 2-propanol degradation [6]. In all cases it was observed that the photocatalytic reaction occurred on Fe$_2$O$_3$ or TiO$_2$ but not on SiC particles corroborating the stability of SiC, but the photocatalytic activity is not high enough. Recently, TiO$_2$ has been deposited on bulk SiC and foam SiC by sol–gel method, Cerneaux et al. [9], and Robert et al. [10], respectively, showing strong adherence of TiO$_2$ on SiC surface. Such results are very promising because such a show indicates that filtering after the photocatalytic process is not necessary.

In this work, TiO$_2$ has been deposited on SiC by sol–gel method, but in order to increase the efficiency of the photocatalytic activity, time deposition has been decreased considerably. SiC–TiO$_2$ has been tested as catalysts for degradation of indigo carmine and methylene blue dyes.

2. Experimental

2.1. SiC–TiO$_2$ synthesis by sol–gel method

SiC–TiO$_2$ were prepared using as raw materials silicon carbide (SiC) commercial powder, mesh 200–450 (Aldrich) and titanium(IV) isopropoxide (Aldrich 99.999%). 3 samples were prepared in order to obtain SiC–TiO$_2$ with different proportions of TiO$_2$, 20, 50 and 80 wt.%, herein labeled as SG1, SG2 and SG3, respectively [9]. First of all, SiC powder was dispersed in 30 mL of ethanol and

* Corresponding author. Tel.: +52 81 8329 4000x7230; fax: +52 81 8376 0477.
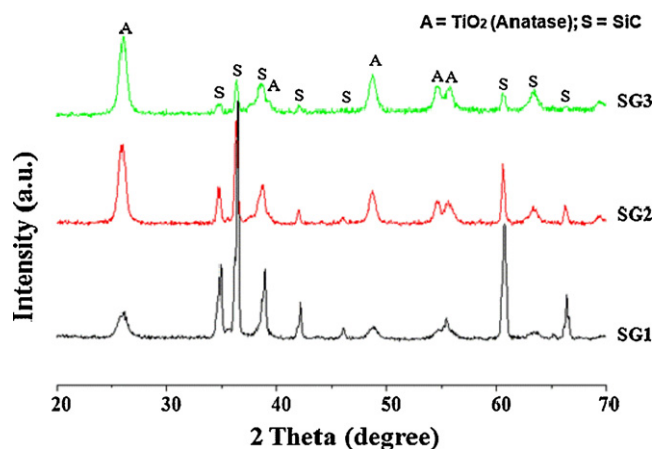E-mail address: isajua13@yahoo.com (I. Juárez-Ramírez).

Fig. 1. XRD patterns of SiC–TiO$_2$ samples prepared by sol–gel method and after thermal treatment at 450 °C during 2 h. SG1, SG2 and SG3 with TiO$_2$ content of 20, 50 and 80 wt.%, respectively.

Table 1
Energy band gap (Eg) and specific surface area (S_{BET}) of SiC–TiO$_2$ catalysts.

Sample	S_{BET} (m^2 g^{-1})	Eg (eV)
SG1	22	3.06
SG2	22	3.06
SG3	25	3.05
TiO$_2$ (P25)	55	3.2

365 to 410 nm). A solution containing 150 mL of methylene blue (20 ppm) or indigo carmine (20 ppm) and 150 mg of catalyst were placed into a quartz reactor under dark condition to reach the adsorption equilibrium. After that, UV-lamp was turn on and reaction was started. Prior to irradiation, the mixture was placed in ultrasound for 5 min. Advance of the photocatalytic reaction was followed by means of UV–vis analysis; samples were taken at different times and the particles catalysts were removed by centrifugation at 5000 rpm for 30 min and then recovered with a 0.22 mm Millipore GV filter. In the same way, total organic carbon (TOC) was measured by total carbon analyser SHIMADZU 5000A.

3. Results and discussion

3.1. Synthesis and characterization

Fig. 1 shows the XRD patterns of SiC–TiO$_2$ samples prepared by sol–gel method and after thermal treatment at 450 °C. According to XRD results, the presence of only TiO$_2$ (anatase phase) and SiC is detected in all samples. The presence of anatase is more evident as the amount of TiO$_2$ increases (SG3 > SG2 > SG1), while intensity of SiC peaks decreases as SiC content decreases. It is notorious to note the absence of rutile phase, which normally appears during thermal treatment above 400 °C [12], therefore in this case we assume that the soft conditions used for the synthesis of TiO$_2$ allow to avoid the appearance of rutile phase. In addition, the absence of secondary phases indicates that there is no chemical reaction between SiC and TiO$_2$ during the sol–gel process and after thermal treatment at 450 °C.

Fig. 2 shows FE-SEM micrographs where the presence of TiO$_2$ nanoparticles deposited on SiC surface is observed; TiO$_2$ particle size is lower than 100 nm. Furthermore, it is observed that due to physical attraction TiO$_2$ nanoparticles form agglomerates on SiC surface. However TiO$_2$ nanoparticles still remain distributed on the surface of SiC.

3.2. Energy band gap (Eg) and specific surface area (S$_{BET}$) measurements

Table 1 shows the energy band gap and specific surface area values for each one of the samples. According to these results, all
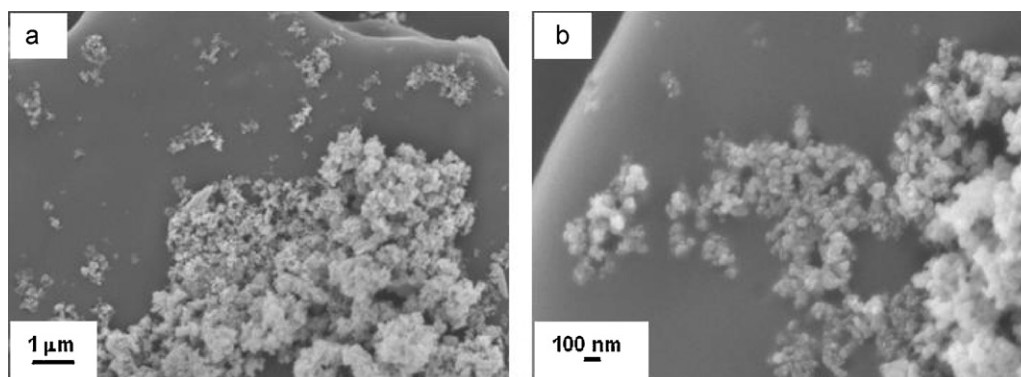
then was sonicated for 15 min. After that, this solution was placed in a reflux system at 70 °C and titanium isopropoxide was added slowly (1 drop/min) to achieve the amount of TiO$_2$ desire. During this process, the system was kept in agitation to have a homogeneous solution. Immediately a mixture of water/acetic acid (55 wt.% ratio) was added in order to promote the hydrolysis–condensation process; after this step, the reaction was kept for 1 h in agitation. The formed gel was dried below 80 °C for 5 h. Finally, dry powder was milled and thermal treatment at 450 °C for 2 h.

2.2. Characterization and photophysical properties

Structural characterization was carried out by X-ray powder diffraction (XRD) using a Bruker D8 Advance diffractometer with CuKα radiation (λ = 1.5406 Å). Particle shape and size were determined by field emission scanning electron microscope (FE-SEM) in a JSM 6700F; prior to the analysis, the powder was placed in an aluminum sample holder and then positioned into the FE-SEM chamber. The energy band gap (Eg) was determined by the Kubelka–Munk function using a UV–vis spectrophotometer (Lambda 35 Perkin Elmer Corporation) coupled with an integrating sphere. Specific surface area (S_{BET}) was measured by N$_2$ physisorption through the BET method using Quantachrome NOVA 2000e equipment.

2.3. Photocatalytic evaluation

Photocatalytic tests were carried out in a quartz tube (500 mL) with a UV-lamp (1.24 mW/cm^2, with wavelength interval from

Fig. 2. FE-SEM micrographs of SiC–TiO$_2$ catalyst after thermal treatment at 450 °C for 2 h (sample SG3). (a) and (b) with different magnifications.
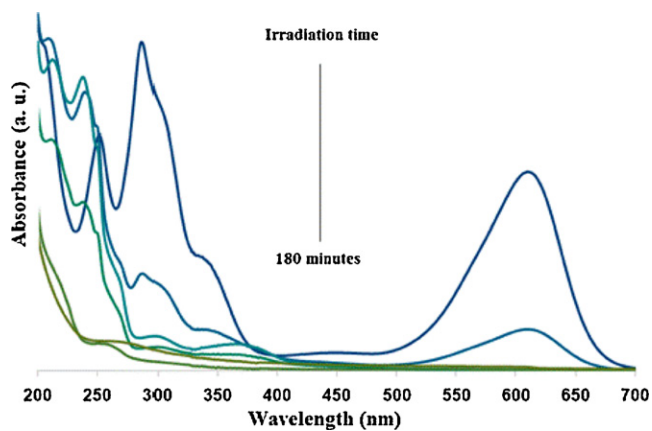
Fig. 3. UV–vis absorption spectra for degradation of indigo carmine using SiC–TiO$_2$ catalysts (SG3).

Fig. 5. TOC analysis for degradation of indigo carmine using SiC–TiO$_2$ prepared by sol–gel and thermal treated at 450 °C.

compounds could be activated efficiently in photocatalytic processes using UV-light because their Eg values are near to 3.0 eV. The small difference observed in band gap values of SiC–TiO$_2$ catalysts is due to the step formed between both semiconductors as a consequence of their different potential oxidation values. This could enhance the photocatalytic behavior for degradation reactions because a synergy effect in SiC–TiO$_2$ catalysts could happen as Yamashita et al. mentioned in a previous work [6]; the electrons will be promoted in the valence and conduction band of both semiconductors, SiC and TiO$_2$.

On the other hand, surface area results indicated that independent of the amount of TiO$_2$ deposited on the surface of SiC, all samples showed values in the same order of magnitude, around 22–25 m^2 g^{-1}. These values are lower than the reported for commercial TiO$_2$ (50 m^2 g^{-1}); however, it is still high enough to consider these materials for their use as photocatalyts in REDOX reactions.

3.3. Photodegradation of indigo carmine

In Fig. 3, a drastic intensity change in the UV–vis absorption spectra when indigo carmine is photodegraded by SiC–TiO$_2$ catalyst (SG3) is observed. According to the UV–vis absorption spectra we assume that a complete degradation of indigo carmine is occurring and it is following a mechanism similar to the one reported by Vautier et al. where several intermediates are formed before it is degraded to CO$_2$ and H$_2$O [13].
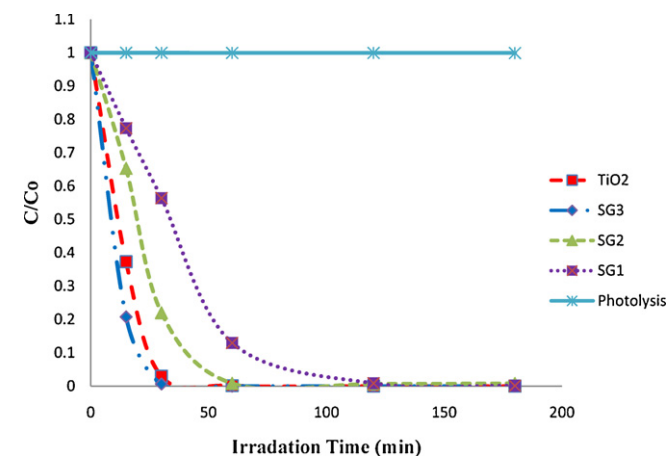

Fig. 4. Photocatalytic curves for degradation of indigo carmine using SiC–TiO$_2$ prepared by sol–gel and thermal treated at 450 °C.
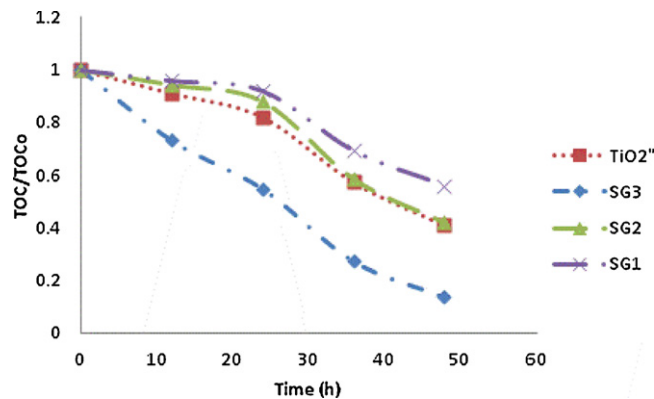
Fig. 4 shows the photodegradation curves for indigo carmine using SiC–TiO$_2$ samples (SG1, SG2 and SG3) and TiO$_2$ (P25). It is observed that activity increases as the amount of TiO$_2$ increases. Sample SG3 containing 80 wt.% TiO$_2$ and 20 wt.% SiC reached almost 100% of degradation of indigo carmine after 30 min of UV irradiation as well as TiO$_2$ (P25), while samples SG1 and SG2 require 100 and 60 min respectively, to achieve same result.

On the other hand, the mineralization process from a photocatalytic degradation reaction could occur through the photo-Kolbe decarboxylation reaction, which involves the reaction of carboxyl radicals with a valence band hole. Commonly the carboxyl anion can be associated with the dye, colored intermediates, aromatic intermediates, or aliphatic organic compounds. Particularly, organic dyes degradation results in the formation of intermediates, which can undergo several reactions leading to mineralization [14].

In our case the conversion of the organic intermediates to CO$_2$ during the indigo carmine degradation at the end of 50 h using SG1, SG2, SG3 and TiO$_2$ (P25) as catalysts follows a similar tendency than the decolorization process. Particularly, SG3 shows the highest mineralization rate of the dye, inclusively better than TiO$_2$ (P25). Therefore the order of mineralization of the material is as follows: SG3 > TiO$_2$ (P25) > SG2 > SG1. This result corroborates that not only the chromophore group is attacked during the photocatalytic reaction but also the nitrogen group and the aromatic group are suffering degradation under UV light (Fig. 5).

3.4. Photodegradation of methylene blue

In Fig. 6 it is evident that the intensity of the absorption bands, 670 and 620 nm, is decreasing gradually as the time increases, indicating that methylene blue is suffering a degradation during the photocatalytic reaction under UV-light irradiation.

Fig. 7 shows the curves of photodegradation of the methylene blue using as catalysts SiC–TiO$_2$ samples (SG1, SG2 and SG3) and TiO$_2$ (P25). It is clear in all cases a similar behavior during the photocatalytic reaction where it was observed that all samples showed better degradation than TiO$_2$ (P25). Sample SG3 containing 80 wt.% TiO$_2$ and 20 wt.% SiC is showing the highest activity, reaching almost 52% of degradation of methylene blue in 180 min under UV-light irradiation. Whereas, sample SG1 containing just 20 wt.% TiO$_2$ and 80 wt.% SiC is achieving 45% of degradation of methylene blue degradation. These results are interesting considering that using SiC as substrate possibly has an activity better than TiO$_2$ (P25) (45% vs 38%) under similar conditions. Methylene blue degradation percentage in this work using SiC–TiO$_2$ catalysts is lower than those reported in previous works related to methylene blue degradation using TiO$_2$ as catalyst [14–20], however in our
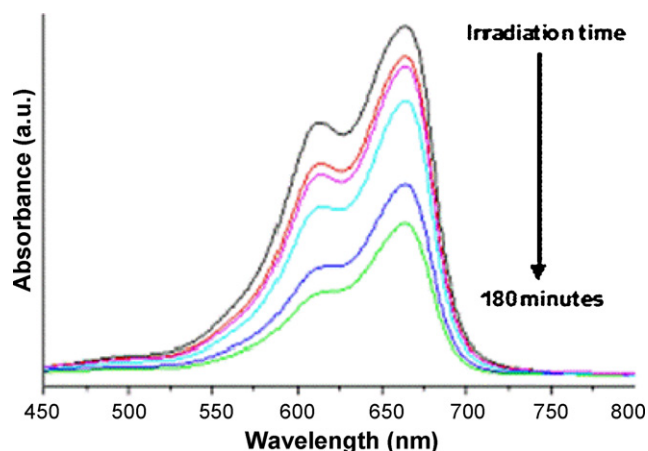
Fig. 6. UV–vis absorption spectra for degradation of methylene blue using SiC–TiO$_2$ catalysts (SG3).

Fig. 8. Final percentages of photodegradation of methylene blue using SiC–TiO$_2$ as catalysts.

case SiC–TiO$_2$ catalysts were irradiated with a lamp power of low intensity (20 W), with wavelength interval from 365 to 410 nm.

According to our results, the photocatalytic activity cannot be attributed to the energy band gap or the specific surface area values. Mainly considering that TiO$_2$ supported on SiC surface showed only the anatase phase and thus its activity should be lower than TiO$_2$ (P25) because it is well known that activity of TiO$_2$ (P25) is due to the mixture of anatase and rutile phases, 80% and 20%, respectively. Therefore this increment on activity may be due to a synergy effect between SiC and TiO$_2$ particles. In this case, due to the sol–gel method used to prepare the SiC–TiO$_2$ catalysts, TiO$_2$ nanoparticles are well dispersed onto SiC surface allowing the transfer of electronic charges between SiC and TiO$_2$ semiconductors, which avoid the fast recombination of the electron–hole pair. We assume that this effect is similar to the study reported by Yamashita et al. [6], where the difference of the energy band gap of each one of the semiconductors causes the presence of a step where the electrons will be promoted in the valence and conduction band of both semiconductors, SiC and TiO$_2$. For an assessment of the degradability of dye wastewaters, the structure of the dye plays a crucial role to determine the effectiveness of the photocatalytic system which attacks the functional groups in order to disrupt the aromatic ring of the dye. In our case the degradation of indigo carmine that is an anionic dye is relatively easier to compare with the methylene blue that is a cationic dye, probably due to the N,N-deethylation reaction [14,21].
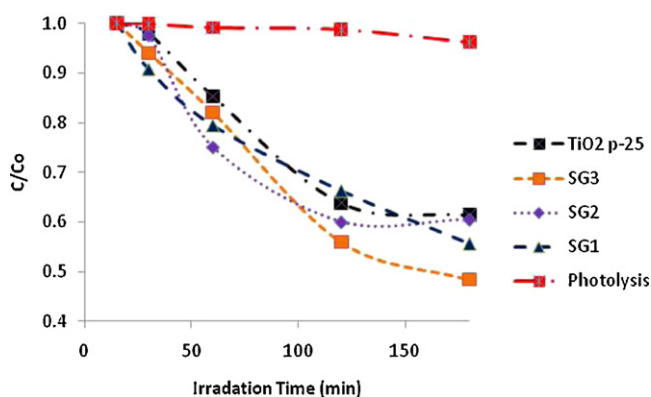
Final percentage of degradation of methylene blue using SiC–TiO$_2$ samples and TiO$_2$ (P25) is showed in Fig. 8. As mentioned above, we assume that the activity is due to a synergy effect between SiC and TiO$_2$ particles. This is due to the sol–gel method used, which allows a good dispersion and attachment of TiO$_2$ particles on the surface of SiC.

Due to the weight of SiC particles, after the photocatalytic reaction is finished, catalysts are settled down and easily separated by simple decantation in one step.

The kinetic parameters for the photocatalytic degradation of indigo carmine and methylene blue dyes were calculated assuming that the reaction follows a first order mechanism. The calculated values reported in Table 2 indicate that sample SG3 is showing the lowest half time life ($t_{1/2}$) in the photodegradation of both dyes. It is clear that SiC–TiO$_2$ catalysts are showing better performance than TiO$_2$ (P25) during the photocatalytic reactions. Thus we assume that a synergy between SiC and TiO$_2$ semiconductors is occurring, favored by the sol–gel method.

According to our results, it is evident in this system that sample SG3 containing 80 wt.% TiO$_2$ and 20 wt.% SiC exhibits the best photocatalytic performance in the degradation of organic dyes under UV-light. Indigo carmine is suffering a faster degradation than methylene blue dye under similar conditions.

Recently TiO$_2$ has shown an important activity for organic dyes degradation, specifically for methylene blue and indigo carmine dyes. However its activity depends on the use of high intensity UV-lamps, the presence of agent dopants, immobilization in a polymeric matrix, or use of particles with different morphologies obtained by different synthesis methods [14–20], see Table 3. Particularly, in this work the use of SiC as support enhanced the activity of TiO$_2$ for methylene blue and indigo carmine degradation under UV light irradiation using a lamp power of low intensity (20 W). In addition the presence of SiC allowed the easy recovering of SiC–TiO$_2$ catalysts after the photocatalytic process.

For industrial applications like waste-water treatment, we consider that our results are very interesting because two situations

Fig. 7. Photodegradation curves of methylene blue using SiC–TiO$_2$ catalysts prepared by sol–gel and thermal treatment at 450 °C.
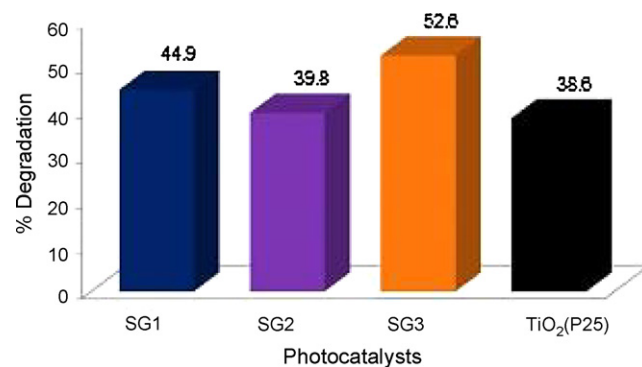
Table 2
Kinetic parameters for indigo carmine and methylene blue photodegradation using SiC–TiO$_2$ as photocatalysts.

Sample	Indigo carmine photodegradation		Methylene blue photodegradation	
	k (min^{-1})	$t_{1/2}$ (min)	k (min^{-1})	$t_{1/2}$ (min)
SG1	0.0145	47.58	0.0027	256
SG2	0.026	26.53	0.0025	277
SG3	0.0528	13.06	0.0031	223
TiO$_2$ (P25)	0.0418	16.50	0.0024	288

Table 3
Comparison of obtained photocatalytic activities with published works related to the indigo carmine and methylene blue dyes degradation.

Material	Organic dye	Activity was attributed to	Degradation (%)	Lamp power	References
Nano-TiO$_2$	Indigo carmine	The activity of the CS TiO$_2$ was attributed to the surface charge of the catalysts that promotes specific intermediates to be formed during degradation.	100	125 W	[14]
N-doped nc-TiO$_2$	Methylene blue	The increment of N content and crystalline size is the important point in the photocatalytic activity.	100	1000 W	[15]
Ti–SBA-15	Methylene blue	The calcined mesoporous Ti–SBA-15 showed high BET surface area and high efficiency in photocatalytic degradation of methylene blue.	80	450 W	[16]
TiO$_2$ nanotubes	Indigo carmine	The activity was enhanced due to the acid media (pH 2) where the material was synthesized	100	125 W	[17]
TiO$_2$-coated non-woven	Indigo carmine	The activity of the TiO$_2$ on paper fibers is influenced by pH, photocatalysts surface and the dye structure.	100	125 W	[18]
Three-dimensionally ordered macroporous titania	Methylene blue	The degradation rate of the material was attributed to the interconnected framework structure, which enhances dye diffusion and provides greater accessibility of the active surface sites for photodegradation.	90	8 W	[19]
Nano-TiO$_2$ in mesoporous SBA-15	Methylene blue	The dispersion effect promoted by mesoporous SBA-15 prevents the anatase to rutile phase transformation and crystal grain growth. This improves the degradation activity.	100	125 W	[20]
SiC–TiO$_2$	Methylene blue and indigo carmine	Activity was attributed to the synergy effect between both semiconductors that reduces the recombination rate of the electron–hole pair.	52 100	20 W 20 W	This work This work

can be solved: one is the possibility to have a TiO$_2$ supported catalyst better than TiO$_2$ (P25) for organic dyes degradation in aqueous solution; commonly when TiO$_2$ is supported on any substrate its activity is affected considerably. The other one is the easy recovering of the catalyst; once the photocatalytic reaction is finished, SiC–TiO$_2$ catalyst is settled down immediately and can be removed just by simple decantation in one step in order to be reused again. Therefore, SiC–TiO$_2$ catalysts prepared by sol–gel method could be considered as potential candidates to be used as photocatalysts in REDOX reactions under UV-light.

4. Conclusions

Results obtained here revealed the possibility to have a TiO$_2$ supported catalyst better than TiO$_2$ (P25) for organic dyes degradation in aqueous solution. In addition, SiC–TiO$_2$ catalysts can be easily recovered once finished the photocatalytic reaction because of the heavy weight of SiC particles. Particularly, SiC–TiO$_2$ catalysts prepared by sol–gel method exhibited higher activity than TiO$_2$ (P25) in the photodegradation of indigo carmine and methylene blue. Catalysts activity is due to the well-dispersed TiO$_2$ nanoparticles on the surface of SiC, which induces a synergy effect between both semiconductors that reduces the recombination rate of the electron–hole pair. Finally, SiC–TiO$_2$ catalysts prepared by sol–gel method are potential candidates to be used as photocatalysts in REDOX reactions under UV-light.

References

[1] H. De Lasa, B. Serrano, M. Salaices, Photocatalytic Reaction Engineering, Springer Science + Business Media, LLC, New York, 2005.
[2] U.I. Gayaa, A.H. Abdullaha, Heterogeneous photocatalytic degradation of organic contaminants over titanium dioxide: a review of fundamentals, progress and problems, J. Photochem. Photobiol. C 9 (2008) 1–12.
[3] T. Zhang, T. Oyama, S. Horikoshi, J. Zhao, N. Serpone, H. Hidaka, Photocatalytic decomposition of the sodium dodecylbenzene sulfonate surfactant in aqueous titania suspensions exposed to highly concentrated solar radiation and effects of additives, Appl. Catal. B 42 (2003) 13–24.
[4] N. San, A. Hatiploglu, G. Kocturk, Z. Cinar, Photocatalytic degradation of 4-nitrophenol in aqueous TiO$_2$ suspensions: theoretical prediction of the intermediates, J. Photochem. Photobiol. A 146 (2002) 189–193.
[5] S. Gelover, P. Mondragon, A. Jimenez, Titanium dioxide sol–gel deposited over glass and its application as a photocatalyst for water decontamination, J. Photochem. Photobiol. A 165 (2004) 241–246.
[6] H. Yamashita, Y. Nishida, S. Yuan, K. Mori, M. Narisawa, Y. Matsumura, T. Ohmichi, I. Katayama, Design of TiO$_2$–SiC photocatalyst using TiC–SiC nanoparticles for degradation of 2-propanol diluted in water, Catal. Today 120 (2007) 163–169.
[7] W.A.A.T.S. Ahmed, PhD thesis, University of Duisburg-Essen, Germany, 2011.
[8] N. Keller, V. Keller, F. Garin, M.J. Ledoux, A new TiO$_2$–β-SiC material for use as photocatalyst, Mater. Lett. 58 (2004) 970–974.
[9] S. Cerneaux, X. Xiong, G.P. Simon, Y.B. Cheng, L. Spiccia, Sol–gel synthesis of SiC–TiO$_2$ nanoparticles for microwave processing, Nanotechnology 18 (2007) 055708.
[10] N.A. Kouamé, D. Robert, V. Keller, N. Keller, C. Pham, P. Nguyen, Preliminary study of the use of SiC foam as a photocatalytic support for water treatment, Catal. Today 161 (2011) 3–7.
[11] V. Keller, F. Garin, Photocatalytic behavior of new composite ternary system: WO$_3$/SiC–TiO$_2$. Effect of the coupling of semiconductors and oxides in photocatalytic oxidation of methylethyketone in the gas phase, Catal. Commun. 4 (2003) 377–383.
[12] C.M. Virginia, L.O. Alejandro, A.E. Alfredo, Influence of the anatase/rutile ratio on the TiO$_2$ photocatalytic activity for the photodegradation of light hydrocarbons, Int. J. Chem. React. Eng. 5 (2007) A92.
[13] M. Vautier, C. Guillard, J.M. Herrmann, Photocatalytic degradation of dyes in water: case study of indigo and of indigo carmine, J. Catal. 201 (2001) 46–59.
[14] R. Vinu, S.U. Akki, G. Madras, Investigation of dye functional group on the photocatalytic degradation of dyes by nano-TiO$_2$, J. Hazard. Mater. 176 (2010) 765–773.
[15] H. Diker, C. Vaelikli, K. Mizrak, A. Dana, Characterization and photocatalytic activity comparisons of N-doped nc-TiO$_2$ depending on synthetic condition and structural different of amine sources, Energy 34 (2011) 1234–1254.
[16] S.K. Das, M.K. Bhunia, A. Bhaumik, Highly ordered Ti–SBA-15: efficient H$_2$ adsorbent and photocatalyst for eco-toxic dye degradation, J. Solid State Chem. 183 (2010) 1326–1333.

[17] L.L. Acosta, A.G.S. Prado, TiO$_2$ nanotubes as recyclable catalyst for efficient photocatalytic degradation of indigo carmine dye, J. Photochem. Photobiol. A 201 (2009) 45–49.

[18] N. Barka, A. Assabbane, A. Nounah, Y.A. Ichou, Photocatalytic degradation of indigo carmine in aqueous solution by TiO$_2$-coated non-woven fibers, J. Hazard. Mater. 152 (2008) 1054–1059.

[19] M. Srinivasan, T. White, Degradation of methylene blue by three-dimensionally ordered macroporous titania, Environ. Sci. Technol. 41 (2007) 4405–4409.

[20] J. Yang, J. Zhang, L. Zhu, S. Chen, Y. Zhang, Y. Tang, Y. Zhu, Y. Li, Synthesis of nano titania particles embedded in mesoporous SBA-15: characterization and photocatalytic activity, J. Hazard. Mater. 137 (2006) 952–958.

[21] A. Houas, H. Lachheb, M. Ksibi, E. Elaloui, C. Guillard, J.M. Herrmann, Photocatalytic degradation pathway of methylene blue in water, Appl. Catal. B 31 (2001) 145–157.